COMPARISON OF ON-ORBIT PERFORMANCE OF RATE SENSING GYROSCOPES

Joseph SEDLAK, Joseph HASHMALL, and Vladimir AIRAPETIAN

Computer Sciences Corporation
7700 Hubble Drive, Lanham-Seabrook, MD, USA 20706

Abstract

This work presents results from the study of a large volume of spacecraft flight data pertaining to gyroscope performance. We have examined long and short term trends of gyroscope biases. Three key results are obtained.

First, an exact solution for the time-dependence of the attitude part of the state error covariance, averaged over the three spacecraft axes, is given. This solution is more complete than the usual cubic polynomial for the variance in that it includes coupling among the three gyroscope axes and includes an important term arising from the initial correlations.

Second, several continuous 24-hour spans of gyroscope data are examined to verify the short-term statistical model. This analysis demonstrates that in-flight data can be used to determine the strength of the white noise driving the random walk of the gyroscope bias. This may be useful for postlaunch improvement to the noise model and for diagnosing the health of the gyroscope.

Third, the long-term trends in gyroscope biases show a nearly linear systematic variation over time scales of years. This has been found on three different missions. While the random walk model is adequate as a basis for onboard Kalman filters or for state estimation using relatively short time spans, these trends indicate that some applications could benefit by accounting for the secular changes in the biases. One example is a new gyroscope calibration method that is under development that allows for multi-epoch bias solutions.

1. INTRODUCTION

This paper presents results of analyses performed by Computer Sciences Corporation for NASA Goddard Space Flight Center (GSFC). The analyses use flight data taken from several missions supported by NASA/GSFC. The purpose is primarily to improve our understanding of rate-sensing gyroscope performance. We address two questions concerning the gyro statistical model: how can the noise parameters be determined in flight, and does the statistical model continue to hold over very long time spans? Preliminary to examining these questions, we discuss the time evolution of the state covariance. This indicates how the uncertainties in the estimated attitude and gyro bias grow and includes important terms that are often neglected.

Gyroscopes often are used onboard spacecraft to measure rotation rates needed for attitude control. The rates can also be used in ground-based processing for determining the spacecraft attitude. A rate-sensing gyroscope provides the data needed for propagating the attitude between sensor observations (e.g., star tracker observations). To obtain optimal estimates of the attitude, knowledge of the noise statistics is needed. Once a statistical model is given, the optimal weights in a Kalman filter, for example, are a function of the strength of the noise sources.

Gyro biases often are estimated along with the spacecraft attitude since they tend to drift significantly with time. (This time may be days or months, depending on mission requirements

This work was supported by the National Aeronautics and Space Administration (NASA)/Goddard Space Flight Center (GSFC), Greenbelt, MD, USA, Contract GS-35F-4381G, Task Order no. S-32415-G.

International Symposium on Spaceflight Dynamics, Biarritz, France, June 2000.

and the quality of the gyros.) The usual gyro noise model includes a random walk of the biases. This is a convenient and simple way to indicate a slow growth in their uncertainty (which is balanced by the reduction in the uncertainty in a Kalman filter as other sensor data are processed). The first question addressed here is whether the strength of the noise driving the bias random walk can be determined using flight data. The noise parameters are usually determined on the ground before launch. On-orbit determination provides verification that the prelaunch values have not changed due to launch shock or aging. If changes are found, the trend can help diagnose problems or predict the eventual sensor failure. Some previous attempts at in-flight determination of the noise parameters have either partially failed due to sensitivity to other sensor errors [Filla 1990], or were limited in their applicability [Lee 1994]. Some of the difficulties in this earlier work may also have come from their neglect of the attitude/bias initial correlation in the covariance evolution equation. This additional term is given specifically in Section 3.

The second question is whether the random walk gyro bias model continues to be useful over very long time spans. This question is driven by a desire to use data from widely separated times to perform gyro calibration. Calibration software often makes use of data from a sequence of attitude maneuvers usually performed over a few hours or a few days. It is often assumed that the calibration parameters, including the biases, remain constant for this time. We are developing a new algorithm for gyro calibration that can use data from multiple batches separated by any amount of time. A separate bias is estimated for each batch, allowing for more accurate calibration of the other, constant parameters (in particular, the scale factors and misalignment).

Section 2 of this paper presents a specific gyro statistical model. This is followed in Section 3 by a derivation of the time evolution of the attitude covariance. The uncertainty in the propagated attitude grows with time due to the noise terms in the gyro model. As mentioned above, the system state is often taken to include both the attitude and the gyro bias. The error covariance of the full state is used in Kalman filters onboard or on the ground for attitude estimation; having an explicit expression for the attitude part of the covariance is useful for spacecraft error budget analyses.

Section 4 analyzes bias statistics and trends for various missions. The main focus is on the Upper Atmosphere Research Satellite (UARS), but results are also given for the Extreme Ultraviolet Explorer (EUVE) and the Rossi X-Ray Timing Explorer (RXTE). Short term trends are analyzed using twelve 24-hour UARS data sets. We show that this data can be used to determine the gyro bias white noise strength, avoiding many of the difficulties in [Filla 1990] and [Lee 1994]. Section 4 also presents plots of long-term trends in the gyro biases. These indicate secular terms that are not part of the gyro model. These terms are small and are not significant for most attitude determination and control purposes. However, the bias trends do indicate the value of allowing for time-dependent biases in gyro calibration applications that extend over very long time spans.

2. GYROSCOPE MODEL

The sensor is composed of three rate-sensing gyroscopes. Each of these is sensitive to rotation about the two axes perpendicular to its spin axis. The three gyros are combined into an Inertial Reference Unit (IRU) where the geometry is chosen to give redundant sensitivity about each axis.

The sensor model describes how the IRU responds to actual rotation of the spacecraft body in inertial space. None of the details of the internal dynamics, electronics, or control feedback are included in this level of modeling. Instead, the sensor output is taken to be a linear transformation of the true rotation rate, with allowance for biases and statistical noise. The model is taken from that given by Farrenkopf [Farr 1974].

The output observations are modeled as the projection of the true rotation rate projected onto the three sensitive axes of the IRU, corrected for any known a priori scale factor error and bias, then rotated into the body frame. To this is added a white noise process representing the inherent sensor errors that accumulate as a random walk of the integrated rotation angle. The scale factors and sensor alignment are assumed in this paper to be accurately known. However, since the biases are known to drift slowly over time, they are also modeled with a random walk process. Thus,

$$\begin{aligned} \vec{\omega} &= \vec{u} - \vec{b} - \vec{\eta}_1 \\ \frac{d\vec{b}}{dt} &= \vec{\eta}_2 \end{aligned} \tag{1}$$

where $\vec{\omega}$ is the true rate vector with magnitude ω, $\vec{u}$ is the measured rate vector after accounting for the a priori data adjustments, $\vec{b}$ is the bias correction vector, and the η terms are white noise sources driving random walk of the rotation angle and bias. The 2-time expectation values are

$$E\left[\vec{\eta}_1(t)\vec{\eta}_1^T(t')\right] = \begin{pmatrix} \sigma_{1,x}^2 & 0 & 0 \\ 0 & \sigma_{1,y}^2 & 0 \\ 0 & 0 & \sigma_{1,z}^2 \end{pmatrix} \delta(t-t')$$

$$E\left[\vec{\eta}_2(t)\vec{\eta}_2^T(t')\right] = \begin{pmatrix} \sigma_{2,x}^2 & 0 & 0 \\ 0 & \sigma_{2,y}^2 & 0 \\ 0 & 0 & \sigma_{2,z}^2 \end{pmatrix} \delta(t-t') \tag{2}$$

where δ is the Dirac delta-function, and the σ_1 and σ_2 are the strengths of the white noise sources allowing for differing values on all 3 gyro axes. As an example, the Teledyne DRIRU-II gyros [GSFC 1976], as flown on UARS and EUVE, are specified to have inherent noise of roughly $\sigma_1^2 \approx 10^{-14}$ rad^2/sec and $\sigma_2^2 \approx 10^{-20}$ rad^2/sec^3 (the σ_1 and σ_2 are called σ_v and σ_u in [Farr 1974] and some other references). These noise values are from the DRIRU-II specifications for time spans up to 1 month. Beyond 1 month, the propagated attitude and bias errors may well show trends that deviate from this random walk model.

3. TIME EVOLUTION OF THE COVARIANCE

In this Section, the covariance of the error state vector is examined and its evolution equation is given. The covariance is broken down into submatrices that obey coupled equations. The gyro bias covariance as a function of time is easily obtained. Finding an exact expression for the attitude covariance is a little more difficult. It can be derived from the continuous-time form of the equations by solving the coupled equations for the bias, then the correlations, and finally the attitude covariance. Alternatively, it can be obtained starting from the known discrete-time-increment expression for the entire state error covariance. The latter method is presented here; it is somewhat briefer since it assumes knowledge of the transition matrix. For background material, for example, see [Gelb 1974] for a general discussion of the covariance evolution, or [Lefferts 1982] for specific application to the spacecraft attitude/gyro bias problem.

The main result of this Section is to show how the attitude uncertainty grows with time. The result is given below in Eq. (15). The leading terms indicate that the mean variance grows as a cubic polynomial. (The mean variance is obtained by taking one-third of the Trace of the attitude

part of the covariance matrix to average over the three spacecraft axes.) If the attitude errors can be determined from in-flight observations, this polynomial can be fit to determine the gyro noise parameters. However, it is difficult to determine the true attitude error and to distinguish gyro propagation error from the influence of small systematic errors in the various attitude sensors. The cubic term (which gives the gyro bias random walk) is particularly hard to fit reliably. Even with a good determination of the attitude error, difficulties arise from the uncertainty in the initial attitude/bias correlation term which enters Eq. (15) with a linear time-dependence and from the coupling among the axes due to spacecraft motion. The purpose of this Section is to make these terms explicit by giving the exact solution for the mean attitude variance.

Let the error state vector, x, consist of attitude and gyro bias corrections [Lefferts 1982]. The state evolution equation then is $dx/dt = Fx$, where the evolution matrix is

$$F = \begin{bmatrix} -\tilde{\omega} & I_{3\times3} \\ 0_{3\times3} & 0_{3\times3} \end{bmatrix} \tag{3}$$

and I is the identity matrix. For any 3-component vector, define the skew symmetric matrix to be

$$\tilde{\omega} \equiv \begin{pmatrix} 0 & -\omega_z & \omega_y \\ \omega_z & 0 & -\omega_x \\ -\omega_y & \omega_x & 0 \end{pmatrix} \tag{4}$$

Combining the noise terms from Eq. (2), the gyro noise spectral density matrix is

$$Q(t) = \begin{bmatrix} \sigma_{1,x}^2 & 0 & 0 & 0 & 0 & 0 \\ 0 & \sigma_{1,y}^2 & 0 & 0 & 0 & 0 \\ 0 & 0 & \sigma_{1,z}^2 & 0 & 0 & 0 \\ 0 & 0 & 0 & \sigma_{2,x}^2 & 0 & 0 \\ 0 & 0 & 0 & 0 & \sigma_{2,y}^2 & 0 \\ 0 & 0 & 0 & 0 & 0 & \sigma_{2,z}^2 \end{bmatrix} \tag{5}$$

The state error covariance matrix, P, evolves according to the equation

$$\frac{dP}{dt} = FP + PF^T + Q(t) \tag{6}$$

See, for example, [Gelb 1974]. The discrete-time formulation of Eq. (6) is

$$P_k = \Phi_{k-1} P_{k-1} \Phi_{k-1}^T + Q_{k-1} \tag{7}$$

where $P_k = P(t_k)$. The state transition matrix from t_{k-1} to t_k is

$$\Phi_{k-1} = \begin{bmatrix} \phi_{k-1} & \psi_{k-1} \\ 0_{3\times3} & I_{3\times3} \end{bmatrix} \tag{8}$$

and

$$Q_{k-1} = \int_{t_{k-1}}^{t_k} \Phi(t_k, t') Q(t') \Phi^T(t_k, t') dt' \tag{9}$$

We are interested in the growth of the covariance, so take $t_{k-1} = 0$, and $t_k = t$. The transition submatrices from 0 to t_k in Eq. (8) then can be shown to be

$$\phi = \phi(t_k) = e^{-\tilde{\omega} t_k} = I - \frac{\tilde{\omega}}{\omega}\sin\omega t + \frac{\tilde{\omega}^2}{\omega^2}(1-\cos\omega t)$$
$$\psi = \psi(t_k) = \int_0^{t_k} \phi(t')dt' = I\,t - \frac{\tilde{\omega}}{\omega^2}(1-\cos\omega t) + \frac{\tilde{\omega}^2}{\omega^3}(\omega t - \sin\omega t) \tag{10}$$

Divide the covariance matrix into submatrices

$$P = \begin{bmatrix} P_a & P_c \\ P_c^T & P_b \end{bmatrix} \tag{11}$$

representing the 3×3 covariances of the attitude error, the bias vector, and their correlation. Then, the gyro bias part of Eq. (7) yields

$$P_b = P_b^o + \begin{pmatrix} \sigma_{2,x}^2 & 0 & 0 \\ 0 & \sigma_{2,y}^2 & 0 \\ 0 & 0 & \sigma_{2,z}^2 \end{pmatrix} t \tag{12}$$

where the superscript on P_b^o indicates initial value (and similarly below for P_a^o and P_c^o). The linear growth of P_b is characteristic of a random walk. If σ_2^2 is the average of the gyro bias noise for the three gyro axes, then the mean bias variance, averaged over the three axes is

$$\frac{1}{3}Tr\,P_b = \frac{1}{3}Tr\,P_b^o + \sigma_2^2\,t \tag{13}$$

From Eq. (7), the attitude part of the covariance at time t is

$$P_a = \phi P_a^o \phi^T + \psi P_c^{oT} \phi^T + \phi P_c^o \psi^T + \psi P_b^o \psi^T + \int_0^t \left[\phi(t') \begin{pmatrix} \sigma_{1,x}^2 & 0 & 0 \\ 0 & \sigma_{1,y}^2 & 0 \\ 0 & 0 & \sigma_{1,z}^2 \end{pmatrix} \phi^T(t') + \psi(t') \begin{pmatrix} \sigma_{2,x}^2 & 0 & 0 \\ 0 & \sigma_{2,y}^2 & 0 \\ 0 & 0 & \sigma_{2,z}^2 \end{pmatrix} \psi^T(t') \right] dt' \tag{14}$$

The mean attitude variance is obtained by taking the Trace of Eq. (14) and dividing by 3. This is the average attitude error for all three axes with equal weight. Let σ_1^2 be the average random walk noise for the three gyro axes, and assume σ_2^2 is the same on all three axes. This yields

$$\frac{1}{3}Tr\,P_a = \frac{1}{3}Tr\,P_a^o + \sigma_1^2 t + \frac{2}{3}Tr\left(P_c^o \psi\right) + \frac{1}{3}Tr\left(\psi P_b^o \psi^T\right) + \sigma_2^2\left(\frac{t^3}{9} + \frac{4}{3\omega^3}(\omega t - \sin\omega t)\right) \tag{15}$$

exactly. The identities $\psi = \psi^T \phi$, $\psi^T \psi = \psi \psi^T$, $\tilde{\omega} = -\tilde{\omega}^3/\omega^2$, and $Tr\,\tilde{\omega}^2 = -2\omega^2$ can be derived and are useful in arriving at Eq. (15). Expanding the final expression in Eq. (15) shows the expected cubic leading behavior of the σ_2^2 term

$$\sigma_2^2\left(\frac{t^3}{3} - \frac{\omega^2 t^5}{90} + \cdots\right) \tag{16}$$

Note from Eq. (10) that the leading term in ψ is linear in time. This makes the P_c^o term linear with time and the P_b^o term quadratic in Eq. (15). These initial values would need to be known before σ_1 and σ_2 could be determined by a direct fit to the attitude error. Also, if the rotation rate is non-zero, the higher order parts of ϕ and ψ become important. This has the effect of coupling the three gyro axes in Eq. (15).

4. GYRO BIAS TRENDS

The gyro biases presented in this Section were obtained using a batch least-squares, differential-corrector Attitude Determination System (ADS). In this paper, the ADS is used to find the attitude and gyro bias vector that minimizes the root-mean-square differences between observed star tracker vectors in the body frame and catalog star positions in the reference geocentric inertial frame (GCI). The solution state vector represents the best estimate of the attitude and gyro bias at an epoch time, usually taken to be the midpoint of the time span. The star tracker observation errors over the entire time span are obtained by propagating the epoch attitude using the gyro rates corrected with the biases estimated in the previous iteration.

One-Day Variation

Using the results of Section 3, one could try to determine the gyro statistical noise parameters from flight data by studying the growth of attitude error as a function of gyro propagation time. However, the polynomial fit is complicated by uncertainty in the initial error correlations and coupling of the errors on all axes due to spacecraft motion. There can also be temperature variations of the parameters and systematic noise in the other sensors that masquerade as biases. The actual error growth is very small; it is difficult, in particular, to determine the cubic term in the polynomial fit. This is the term that gives the noise strength, σ_2, that drives the gyro bias random walk. This Section shows that this noise can be determined by analyzing the estimated biases themselves rather than the propagated attitude error.

Experience gained from operations support for UARS and similarly equipped missions has shown that the uncertainty in estimated gyro biases is roughly 0.005 arcsec/sec. This is based on either Kalman filter or batch least-squares (differential corrector) methods with input from one orbit of data for gyros and two fixed-head star trackers. Using the specified $\sigma_2^2 \approx 10^{-20}$ rad^2/sec^3, the bias can be expected to walk to 0.005 arcsec/sec in about 60000 sec. (Remember, the random walker travels a net distance with mean of zero but with a standard deviation that grows as the square root of time.) Hence, it is necessary to look at time spans of nearly 1 day in order to see the effect of the bias random walk. (The results given below show both a somewhat smaller initial bias uncertainty and a smaller bias noise than expected.)

An archive of UARS attitude and orbit data from 1992 was collected for analysis. Twelve 24-hour data sets were available. These were broken into 1-orbit batches, and attitudes and gyro biases were obtained for each batch using the ADS software. The orbital period for UARS is maintained at 5772 sec; thus, 14 independent bias estimates were determined on 12 separate days.

The bias changes, or delta-biases, were computed for all possible lag times. That is, the bias changes after 1 orbital period are all collected into one set; the changes after 2 orbital periods are collected in another set, and so on. The distribution functions of these sets are shown in Fig. 1 as a series of histograms. Each histogram pertains to a given time lag, as indicated in orbital periods. Each histogram shows the number of occurrences for several observed delta-biases binned into 20 intervals of size 0.001 arcsec/sec. To improve the statistics, the bias changes on the X-, Y-, and Z-axes are all combined. Note that there are many more samples with lag time of 1 or 2 orbital periods than for 13 or 14 periods. The small number of samples makes the distributions appear less Gaussian for long lag times.

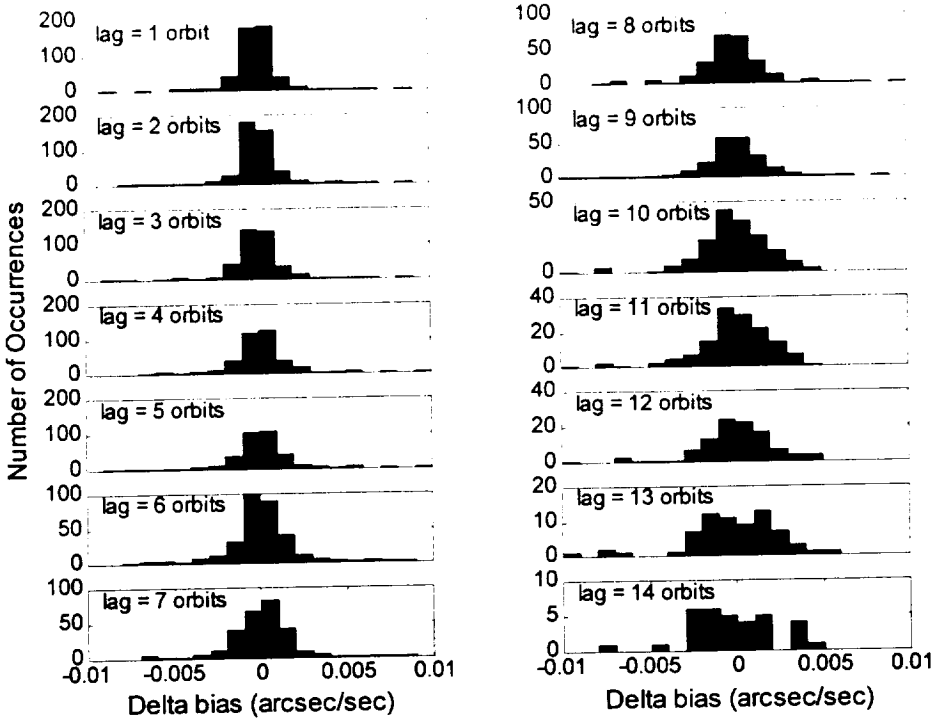

Fig. 1. Distribution functions of gyro bias changes (arcsec/sec) for lag times ranging from 1 to 14 orbital periods (period=5772 sec). Sample consists of twelve 24-hour data sets, and data from the X-, Y-, and Z-axis gyro biases have been combined.

The widths of the distributions in Fig. 1 can be seen to increase as the time lag increases. This is the growth in mean bias variance indicated in Eq. (13). Thus, to determine the value of σ_2^2, one can compute the variance of each distribution in Fig. 1 and fit them to a straight line. The slope is σ_2^2, as shown by Eq. (13).

Figure 2 shows the variances as a function of time lag. Outlying points have been removed from the distributions (see the discussion below). The value of the bias noise obtained from the slope for this example is σ_2 = 8.1e-06 arcsec/sec$^{1.5}$ or σ_2^2 = 1.5e-21 rad^2/sec^3 which is somewhat better than the DRIRU-II specifications.

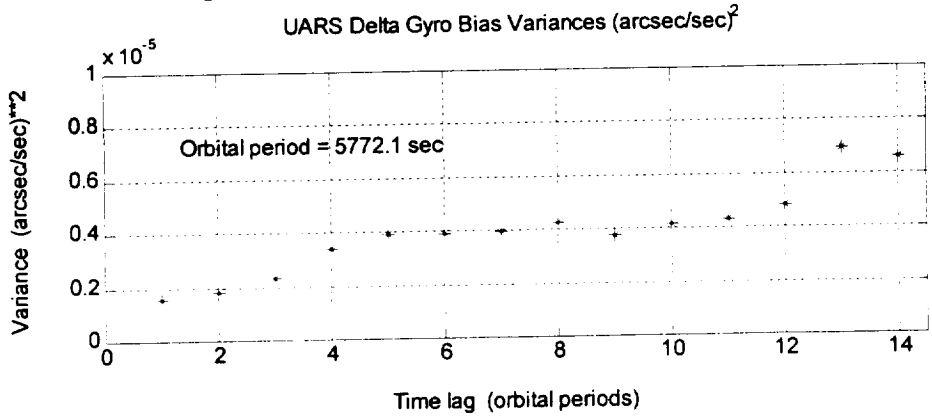

Fig. 2. Variances of gyro bias changes (arcsec/sec)^2 as a function of lag time.

For the longest lag time of 14 orbital periods, there is only one sample for each axis from each of the 12 data sets. It is clear that the statistical sample is much better for the shorter time lags, however the slope is more observable by including the longer time lags. The slope is uncertain by roughly a factor of 2. This number derives from numerical tests using different axes and various shifts and tolerances in the data processing. (Kalman filter performance is robust for changes in σ_2^2 of a factor of 10, so factor of 2 accuracy is quite good enough to be useful.)

One source of error comes from the outliers in the distributions. These make the variance for some time lags to appear too large. It must be remembered that these distributions are for bias changes where the bias error itself was expected to be 0.005 arcsec/sec. The actual error has been reduced from this value by very careful attention to eliminating bad data. The gyro telemetry data were all checked and bad points removed before running the ADS. Careful star identification was done on the star tracker data using a pattern match method. Outliers in the star observations were removed by setting a 3-sigma tolerance when running the ADS (that is, any star observations more than 3 standard deviations from the expected values were discarded). However, the outliers in Fig.1 are testimony to the presence of some small systematic errors. These cause the bias estimates on adjacent orbits to oscillate slightly, so the delta-biases oscillate back and forth, producing the outlying points in the histograms. To avoid this problem, the outliers are removed by imposing a 4-sigma limit. Any delta-biases larger than 4 standard deviations are removed from each histogram, then the variances are re-computed.

The tiny systematic errors that cause a few of the estimated biases to oscillate may be due to temperature changes causing true bias shifts or due to star tracker errors as certain stars with small catalog errors pass through different parts of the star tracker fields of view on subsequent orbits. They could also be due to differences in the star tracker accuracy in various parts of the fields of view, combined with random differences from orbit to orbit in the distribution of stars in the fields of view.

Long-Term Variation

Some long-term trends in gyro biases are shown in Fig. 3. The data represent values from UARS for which we have a more complete history of biases than for any of the other missions studied. Trends for other missions are qualitatively similar.

The data in Fig. 3 represent gyro bias changes over a time span of more than 2.5 years. These biases were computed using the ADS as part of the ongoing UARS mission support in the NASA/GSFC Flight Dynamics Facility.

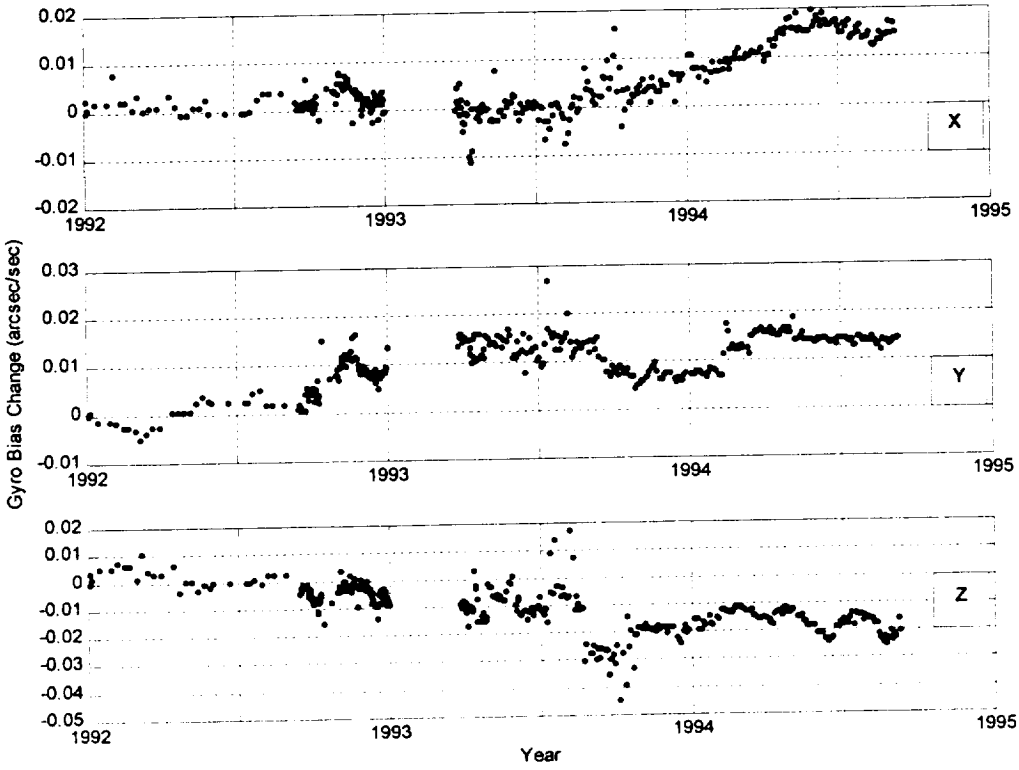

Fig. 3. Change in UARS gyro biases (arcsec/sec) over nearly 3 years.

One problem with the original solutions was that the computed gyro biases had large systematic changes whenever the spacecraft performed a 180 deg yaw maneuver (this maneuver occurred approximately every 5 weeks throughout the mission in order to keep the Sun always on the same side of the spacecraft). These apparent bias changes arise from a small uncorrected misalignment of the gyroscope. This causes the ±1 revolution per orbit Y-axis pitch rotation of the spacecraft to project slightly onto the X- and Z-gyro axes. The X- and Z-axis gyros detect this projection, and the ADS represents it as a new gyro bias.

At other times, the ADS bias solutions showed occasional large, abrupt changes. These shifts occurred whenever the operations personnel recalibrated the gyros and began adjusting the raw rates with new a priori scale factors, misalignments, and biases.

All of these large, systematic shifts in the biases were removed from the trend plots. It was assumed that the bias immediately after each shift equals the bias immediately before the shift. Hence, the shift is removed by offsetting all subsequent biases by the amount of the shift. The overall trend in the biases has a small slope and the time between bias solutions is short (about 1 week), so treating the biases before and after each shift as equal does not introduce much error. The biases were also shifted to make the first value zero so these plots actually represent the change in gyro bias over the course of time. It is the slope which is of interest in this study, not the biases themselves.

The gyro biases shown in Fig. 3 are actually quite stable. The overall drift of the biases is roughly 0.01 arcsec/sec/year. However, the random walk model predicts a spread of biases with standard deviation 5 times larger than this even with the small slope found in Fig. 2.

Similar plots for EUVE show slopes of about the same magnitude as UARS. Both UARS and EUVE carry Teledyne DRIRU-II gyros. The RXTE spacecraft carries Kearfott SKIRU-DII gyros. These are designed to be functionally similar to the DRIRU-II. The slope of the bias trend plot for RXTE shows larger magnitudes of about 0.08 arcsec/sec/year. As seen in Fig. 4, the trend here is more clearly linear. These systematic linear trends show that the random walk model does not apply for long time spans.

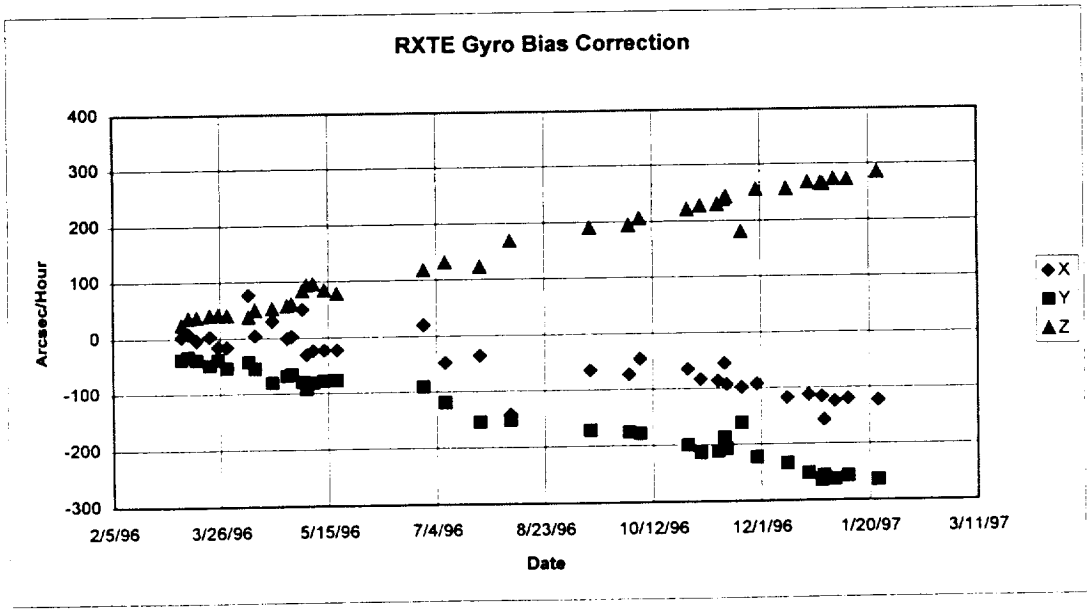

Fig. 4. Change in RXTE gyro biases (arcsec/hour) over nearly 1 year.

5. CONCLUSIONS

In this paper, we have presented an exact closed-form solution of the time evolution of the mean attitude variance subject to the Farrenkopf gyro noise model. The initial correlation term and other error sources cause much difficulty in determining the strength of the gyro bias noise from analysis of the attitude error. It is shown how the gyro bias noise can be determined by analyzing the biases themselves rather than the attitudes.

Long-term plots of the biases show approximately linear trends. This secular drift is not included in the gyro model. The drift is very small for two DRIRU-II units studied and somewhat larger for a SKIRU-DII. The slopes are expected to be much larger for some of the less stable gyros available and may also increase for any unit as it ages. It is suggested that gyro calibration methods that use maneuver data spread out over long time spans can be improved by allowing for a changing bias. Software is under development that solves for the constant gyro scale factor and misalignment corrections simultaneously with multi-epoch attitudes and biases. The advantage of such a method is that it allows ongoing improvement to the gyro calibration parameters with every attitude maneuver, rather than relying on a single campaign of maneuvers specifically for calibration. One may speculate that less stable gyros might also benefit by including the long-term trend into the gyro model and solving for the slope as part of an augmented state vector.

REFERENCES

[Farr 1974] R. L. Farrenkopf, "Generalized Results for Precision Attitude Reference Systems Using Gyros," *AIAA Mechanics and Control of Flight Conference*, AIAA Paper 74-903, Anaheim, California, August 1974.

[Filla 1990] O. Filla, T. Willard, D. Chu, and J. Deutschmann, "Inflight Estimation of Gyro Noise," *Flight Mechanics/Estimation Theory Symposium*, NASA Goddard Space Flight Center, Greenbelt, Maryland, May 1990.

[Gelb 1974] A. Gelb, ed., *Applied Optimal Estimation*, Cambridge: MIT Press, 1974.

[GSFC 1976] "Specification for NASA Standard Inertial Reference Unit," NASA Document, GSFC-S-712-10, Goddard Space Flight Center, Greenbelt, Maryland, May 1976.

[Lee 1990] M. Lee, et al., "Inflight Estimation of Gyro Noise on the Upper Atmosphere Research Satellite (UARS) and Extreme Ultraviolet Explorer (EUVE) Missions," *Flight Mechanics/Estimation Theory Symposium*, NASA Goddard Space Flight Center, Greenbelt, Maryland, May 1994.

[Leff 1982] E. J. Lefferts, F. L. Markley, and M. D. Shuster, "Kalman Filtering for Spacecraft Attitude Estimation," *J. Guidance, Control, and Dynamics*, Vol. 5, No. 5, Sept.-Oct. 1982.